EXPERIMENTAL INVESTIGATION OF RAM ACCELERATOR CONCEPT USING AN OPTICAL PROBE

by

Kelley Ann Scott

A thesis submitted in partial fulfillment
of the requirements for the degree of

Master of Science
in
Aeronautics and Astronautics

University of Washington

1988

Approved by A. Hertzberg
(Chairperson of the Supervisory Committee)

Program Authorized
to Offer Degree Department of Aeronautics and Astronautics

Date 3 August 1988

In presenting this thesis in partial fulfillment of the requirements for a Master's degree at the University of Washington, I agree that the Library shall make its copies freely available for inspection. I further agree that extensive copying of this thesis is allowable only for scholarly purposes, consistent with "fair use" as prescribed in the U.S. Copyright Law. Any other reproduction for any purposes or by any means shall not be allowed without my permission.

Signature Galen N Smith

Date 3 August 1988

University of Washington

Abstract

EXPERIMENTAL INVESTIGATION OF RAM ACCELERATOR CONCEPT USING AN OPTICAL PROBE

by Kelley Ann Scott

Chairperson of the Supervisory Committee:

Professor Adam P. Bruckner

Department of
Aeronautics and Astronautics

A theoretical and experimental program is underway at the University of Washington to explore the acceleration of projectiles to ultra-high velocities using an in-tube ramjet concept, the ram accelerator. This thesis discusses the experimental investigation of luminosity associated with the operation of the thermally choked subsonic combustion ram accelerator. The theoretical models of ram accelerator performance and combustion activity are outlined. A detailed description of the experimental apparatus and facility is presented, and the results of the investigation are provided. The observations are made using an optical probe, and the results are used to substantiate the current model of the combustion region of the ram accelerator concept. In addition, recommendations for further optical investigations are included.

TABLE OF CONTENTS

	Page
Chapter One: Introduction	1
Chapter Two: Theory	4
Ram Accelerator Model	4
Combustion Zone Model/Origin of Luminosity	7
Chapter Three: Experimental Apparatus	10
Optical Probe	10
Amplification System	14
Chapter Four: Discussion of Results	16
Operating Conditions	16
Transducer Signatures	17
Preliminary Results	19
Thermally Choked Activity	21
Detonation Phenomena	23
Chapter Five: Suggested Research	28
Temperature Measurements	28
Spectroscopic Data	29
Oblique Detonation Phenomena	30
Chapter Six: Conclusions	32
List of References	33
Appendix A: Experimental Facility	36
Appendix B: Instrumentation and Data Acquisition System	41

LIST OF FIGURES

Number		Page
1.	Thermally Choked Ram Accelerator Concept	5
2.	Ram Accelerator Combustion Zone	8
3.	Optical Components	11
4.	Optical Probe	12
5.	Amplification System	15
6.	Transducer Signatures	18
7.	Detonation Wave	24
8.	Unstart and Detonation	26
9.	Oblique Detonation Mode	31
10.	Ram Accelerator Facility	37
11.	Projectile Configuration	39
12.	Kistler Pressure Transducer	42
13.	PCB Pressure Transducer	43
14.	Electromagnetic Coil Transducer	44
15.	Monochrometer System	45
16.	Data Acquisition System Schematic	47

LIST OF TABLES

Number		Page
1.	Fiber Optic Specifications	13
2.	Propellant Compostitions	16

ACKNOWLEDGEMENTS

The author wishes to acknowledge the valuable support and guidance of her advisors, Professors Abraham Hertzberg and Adam P. Bruckner; and the generous contributions of Professor Tom Mattick and Dan Lotz, whose expertise and assistance with the amplification system design were greatly appreciated. Many thanks also go to my fellow research students on the ram accelerator project, Alan Kull, Carl Knowlen, Ed Burnham, Al Alvares, and Dai Murikami; and to Professor Phil Malte for his suggestions and support regarding the observation of spectroscopic data. In addition, the author thanks her mother, Ruth Shelley Scott, for her continued support and good wishes.

CHAPTER ONE: INTRODUCTION

At the University of Washington, a theoretical and experimental program is underway to explore the acceleration of projectiles to ultra-high velocities. The concept, the ram accelerator, involves a new method of chemical propulsion. The principles of propulsion are similar to those of a conventional air-breathing ramjet, but the ram accelerator operates in a somewhat different manner. A projectile resembling the centerbody of a conventional air breathing ramjet is launched into a tube containing high-pressure gaseous propellant. The tube acts as the outer cowling of the "ramjet" and the energy release process, i.e., the combustion, travels with the projectile. No fuel is carried on board the projectile. The pressure, composition, chemical energy density, and speed of sound of the propellant are controlled to optimize performance.

Five modes of the ram accelerator concept have been theoretically investigated under the direction of Professors Abraham Hertzberg and Adam P. Bruckner.[1-7] One of these modes, the thermally choked, subsonic combustion mode, has been experimentally validated. Projectile velocities up to ~2400 m/sec have been attained using methane-based propellant mixtures.

A one-dimensional, quasi-steady, inviscid analytic model determines the theoretical performance of the subsonic, thermally choked ram accelerator. This approach has been used to predict the thrust, velocity, and ballistic efficiency of the projectile. Details of the combustion process central to the operation of this propulsion mode have not been included.

Chapter Two presents the model used to analyze ram accelerator performance, the combustion zone model, and the possible sources of luminosity. Chapter Three describes the optical probe and amplification system. Chapter Four contains the results of the investigation for a variety of test conditions. Suggestions for future research, are presented in Chapter Five, and the conclusions drawn for this investigation are provided in Chapter Six. Appendix A contains descriptions of the experimental facility. Associated instrumentation and the data acquisition system are discussed in Appendix B.

CHAPTER TWO: THEORY

A. Ram Accelerator Model

The theoretical performance of the thermally choked subsonic combustion mode of the ram accelerator is analyzed using a one-dimensional, quasi-steady inviscid model of the flow field. A detailed description is presented in Ref. 4; the major features of that model are summarized below. Figure 1 illustrates the various stations of the flow field. Supersonic flow enters the projectile diffuser, forming a series of weak oblique shocks. The flow is assumed to isentropically expand to beyond the diffuser throat. In the diverging portion of the diffuser the flow experiences a normal shock. This shock is observed to be a complex wave system; its overall effect on the flow is approximated using normal shock relations. The subsonic flow behind the shock is assumed to isentropically expand to the full tube area. Heat addition due to combustion chokes the flow behind the projectile. Gasdynamic conservation equations are applied to the control volume bounded by stations 1 and 6 and the tube wall. An ideal equation of state is used with one set of molecular weights and specific heats before combustion, and with one set after combustion. While this simple approach provides a good approximation of the performance characteristics, specifically thrust and velocity, details of the flow field are not included. The normal shock and conical shock systems, the recirculation zone at the projectile base, and the unsteady combustion activity are not analyzed.

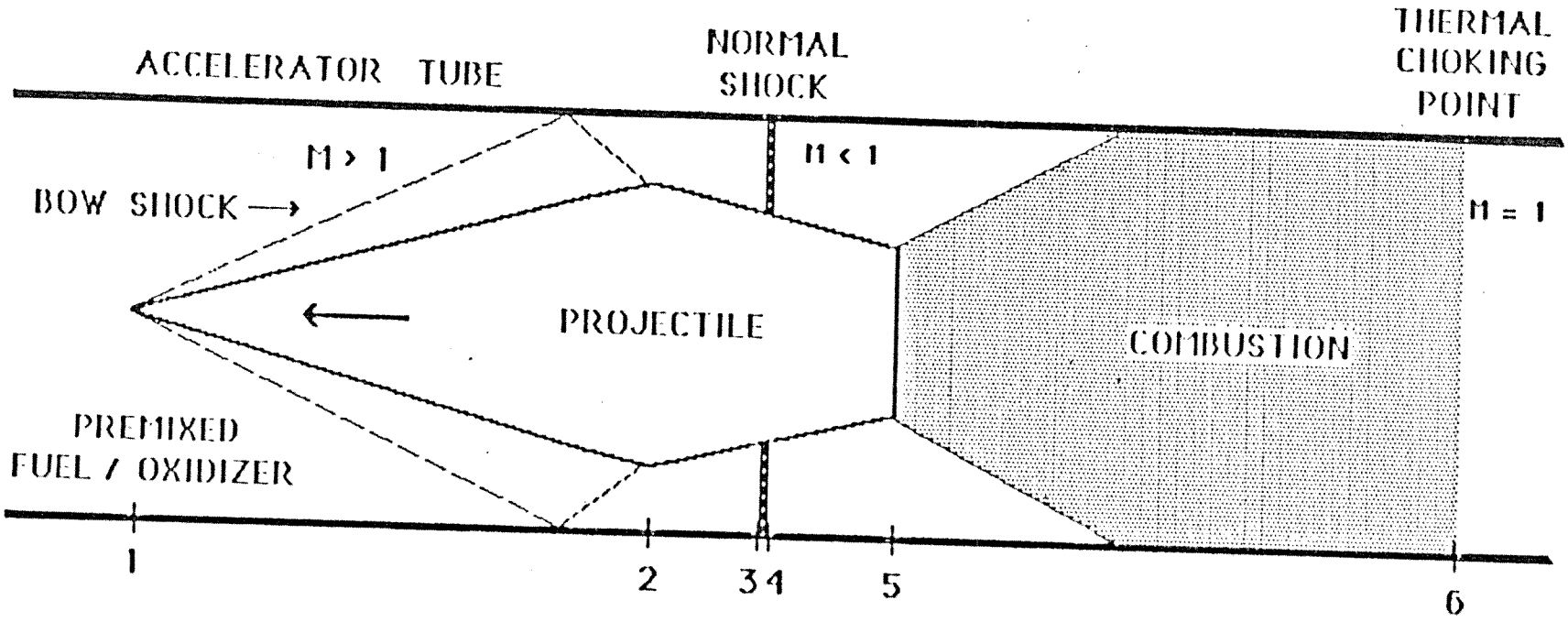

Figure 1 Thermally Choked Ram Accelerator Concept

There are several mechanisms that limit the performance of the ram accelerator. The low velocity limit for a given projectile geometry and propellant mixture is that which allows the normal shock to rest at the throat. The normal shock position is strongly influenced by the projectile velocity or Mach number and by the heat of combustion of a particular mixture. When the projectile velocity exceeds that at which the shock system can remain on the projectile, the shock falls off the projectile and merges with the combustion zone, thus forming a Chapman-Jouguet (C-J) detonation wave. The C-J detonation speed of a mixture is determined to be the maximum possible projectile velocity.[3] The highest practical operating Mach numbers are also limited by the fall-off condition, where the projectile thrust drops to zero. In addition, if the temperature behind the normal shock is sufficiently high to spontaneously ignite the gas, a detonation wave will form, move forward, and unstart the diffuser. An unstart condition is one in which the projectile drives a normal shock or an overdriven detonation wave ahead of itself. This results in rapid deceleration of the projectile. These conditions serve to decrease the maximum projectile velocity in a given mixture to below the C-J detonation speed.[2] The behavior of the combustion zone in relation to these mechanisms can best be observed experimentally, using an optical probe.

Determination of the thermal choke region location is the first step in understanding the combustion zone phenomena. Solution of the gasdynamic equations relating stagnation temperatures in simple-T_0 flow show that the maximum temperature ratio corresponds to the thermal choking, or $M_6 = 1$, condition.[11] Based on a simple analysis of the

critical pressure ratio for the flow field, the location of the thermal choke point is expected where the pressure in the flow field has fallen to roughly half its peak value.[12]

B. Combustion Zone Model/Origin of Luminosity

The combustion region is modeled as a flame stabilized on the blunt rear of the projectile.[2,4] A schematic of this region is shown in Fig. 2.

The recirculation zone is a high-temperature core of the wake of the projectile. Combustion of the pre-mixed gaseous propellant flowing past the projectile begins in the thin shear layer between the free stream flow and the recirculation zone. Generally, combustion is assumed to reach completion at the full tube area. The wake temperature, independent of the overall fluid dynamics, is a function of the chemistry and free stream temperature.[13]

Possible sources of light emission are chemiluminescence, and blackbody radiation from solid carbon, or soot, formed by the combustion of methane- and oxygen-based propellant mixtures. Photoemission from excited molecules such as CO_2^*, C_2^*, or CH_4^* may contribute to the luminosity of the combustion region.[14,15] However, because pressures in this region may reach several hundred atmospheres during thermally choked ram accelerator operation, the chemiluminescence is suppressed.[16] Both the high-pressure environment and the high flame temperatures associated with methane fuels promote the formation of soot in the wake of the projectile.[17] For these reasons, the primary source of luminosity in the subsonic combustion

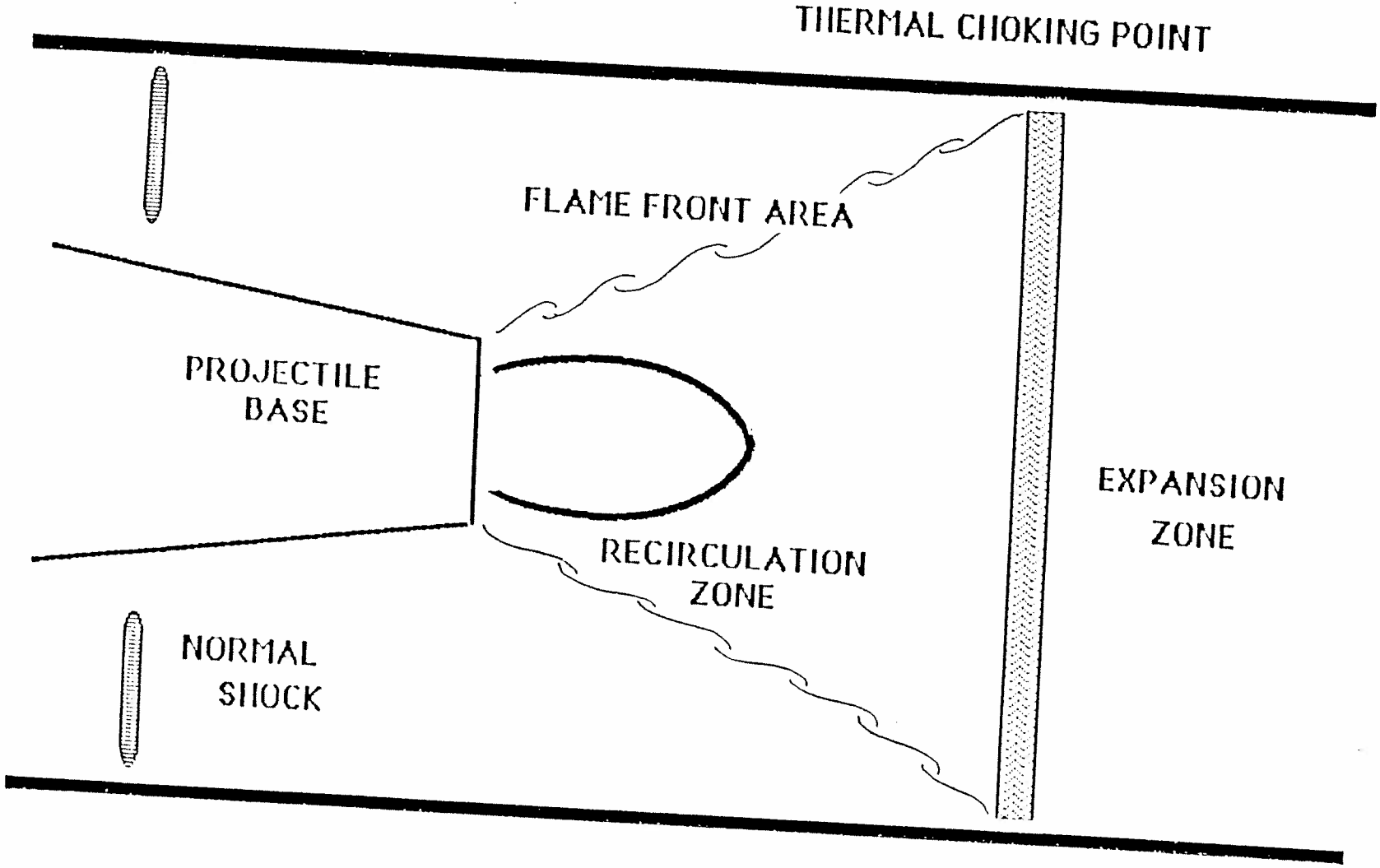

Figure 2 Ram Accelerator Combustion Zone

region is assumed to be the solid carbon. The predominant visible spectral characteristic of diffusion flames and fuel-rich pre-mixed flames is the continuum emission of soot particles.[18]

The flow temperature is greatest in the region of thermal choking. Compression of the propellant gases and chemical heat release combine to bring the flow temperature in the wake of the projectile to ~2000°K or more. Due to extremely efficient heat transfer between the soot particles and the flow, there is a small difference between the flow temperature and the effective radiation temperature.[19,20] Thus the thermal choking region can be identified by the peak in light emission. The light data, correlated with pressure and projectile position data, provide a qualitative view of the entire flow field as well as the physical dimensions of the combustion zone. With the optical probe, it is possible to observe unsteady combustion activity not accounted for in the analytic model. In addition, the temperature itself can be estimated using simple blackbody relations and relative intensities obtained at different wavelengths.[21,22] This will be the focus of future research using the optical probe.

CHAPTER THREE: EXPERIMENTAL APPARATUS

The optical set-up used in the present investigation is shown in Fig. 3. The optical probe and related components are described below, while the experimental facility is discussed in Appendix A. Associated instrumentation, and the data acquisition system are described in Appendix B.

A. Optical Probe

Figure 4 shows the optical probe assembly. The body of the probe is made from 4140 steel. A Lexan window, nominally 5 mm thick, is inserted between the probe aperature and the face of the fiber optic light guide. Although high-transmission windows would be preferable, scratching and cracking of glass windows were expected. Instead, Lexan was selected as the window material because it resists cracking and is easily machined. An "o"-ring seal was incorporated to preclude leakage of the high-pressure combustible gas mixture. To help center the light guide inside the probe, a Lexan sleeve is inserted around the light guide, between the window and inner plug. The probe is easily disassembled for replacement of the window and light guide sleeve. Between tests, the windows are cleaned and replaced. To reduce sooting on the face of the Lexan window, and to provide some spatial filtering of luminosity reflected by the tube wall, the Lexan window was recessed 6 mm into the base of the probe, and an aperture of 0.16 mm was used.

The light guide has a polymethyl-methacrylate core, fluorine polymer cladding, and a black plastic jacket. The diameter of the core is ~1 mm; the outer diameter of the light guide is ~2.2 mm. The acrylic fiber was selected for its flexibility and resistance to

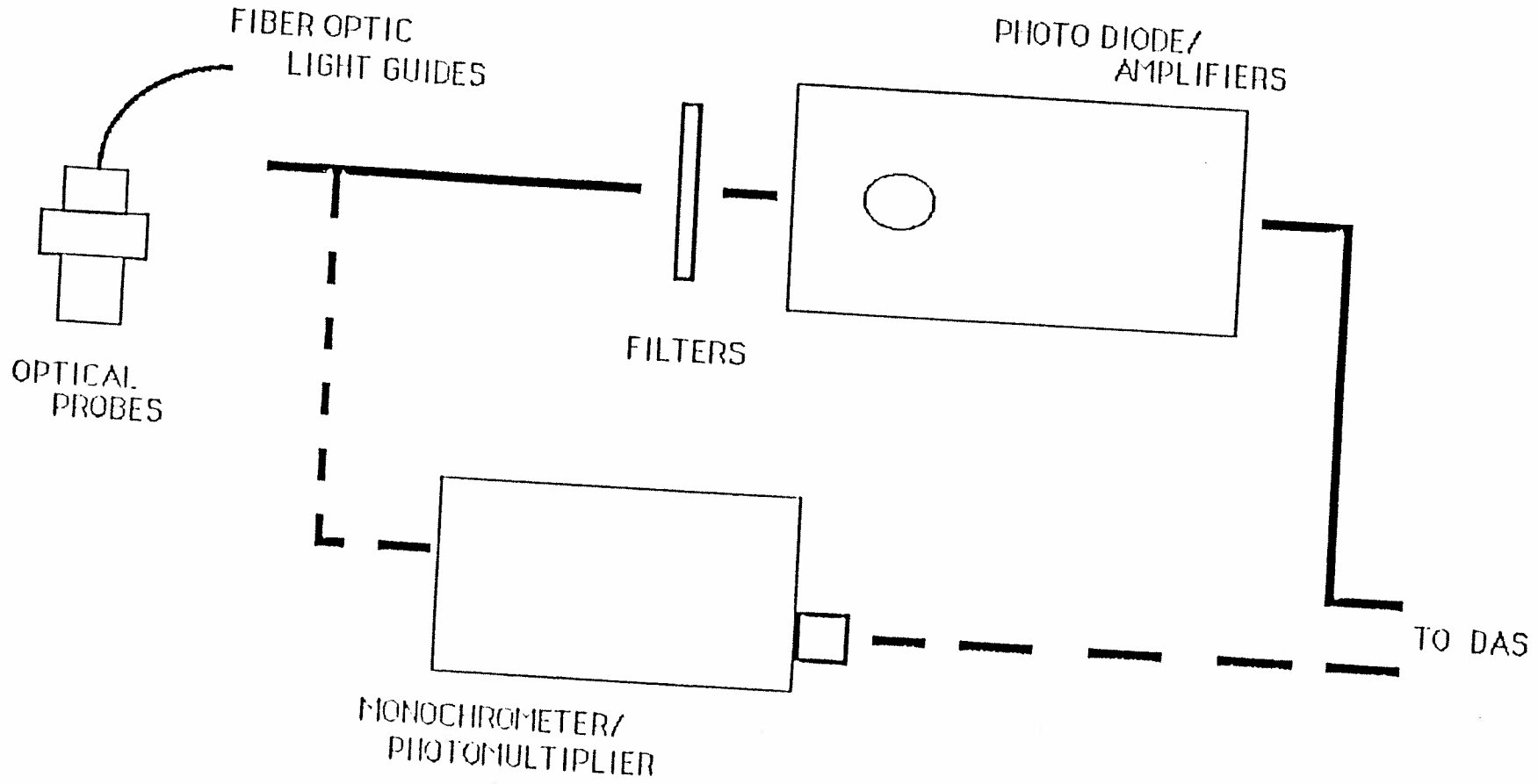

Figure 3 Optical Components

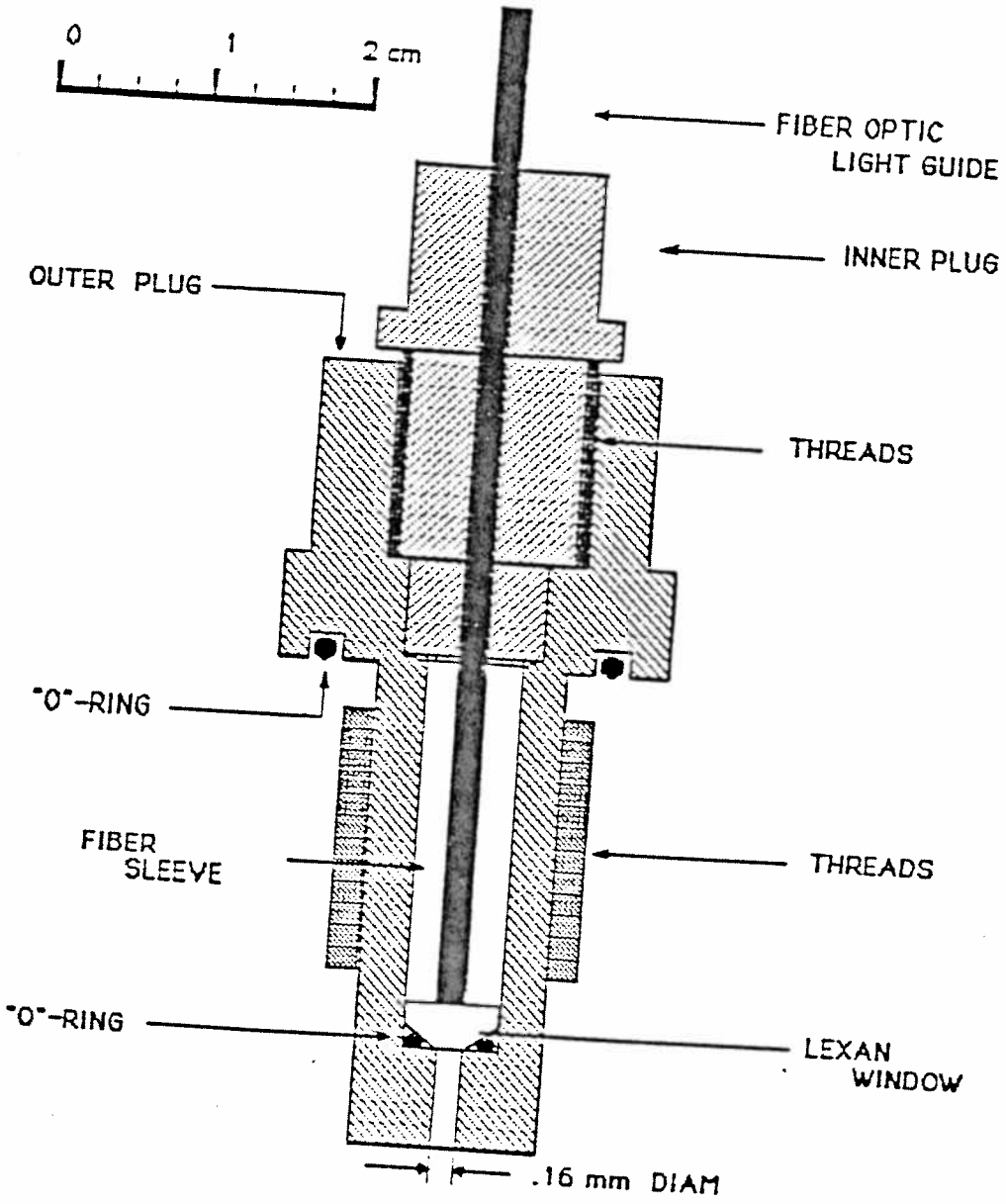

Figure 4 Optical Probe

cracking; the light guides must be removed and replaced between tests. However, the fiber material permits only the transmission of light in the visible spectrum. The fiber conducts luminosity data from the optical probe to a photodetector located a short distance from the instrument port containing the probe. The fiber optic light guide specifications are provided in Table 1.

Table 1: Light Guide Specifications

Core Refractive Index	1.492 (n_1)
Cladding Refractive Index	1.417 (n_2)
Numerical Aperture (NA)	$0.47 \pm 0.03(\sqrt{(n_1)^2-(n_2)^2})$
Acceptance Angle	56° ($2\sin^{-1}(NA)$)
Attenuation	160-250 dB/km at 660 nm

The photodetector is a silicon PIN-type photodiode, RCA model C30808, with a photosensitive surface area of 5 mm^2. This type of detector was selected for its broad spectral range, high responsivity in the visible to near IR regions of the spectrum, and fast time response. The device is most sensitive to wavelengths less than 950 nm.

Attenuation through the Lexan window is the primary cause of transmission losses. The acrylic light guide is responsible for very little of the overall loss. The transmission of the optical probe system is ~40%. While this is not ideal, sufficient light is conducted through the system to accomodate luminosity data collection.

When required, neutral density filters are positioned between the fiber ends and the photodiodes to prevent signal saturation.

B. Amplification System

Using the amplification system illustrated in Fig. 5, the light signals are amplified and directed to the data acquisition system for processing and storage. The amplifier system consists of an operational amplifier (National LM318N) in series with a field-effect transistor (2N5564) to provide fast frequency response and high gain. The system bandwidth is approximately 1 MHz. The voltage output is roughly 75,000 V/W of light input, based on the nominal gain of 150 times the current generated by light striking the photodiode. This estimate is applicable for blackbody radiation at an effective temperature above 2000°K and nominal silicon P-I-N photodiode responsivity in the visible range.

Initial observations were made using an existing amplifier system. This system was bandwidth limited; often very little of the high-frequency characteristics of the luminosity data were obtained.

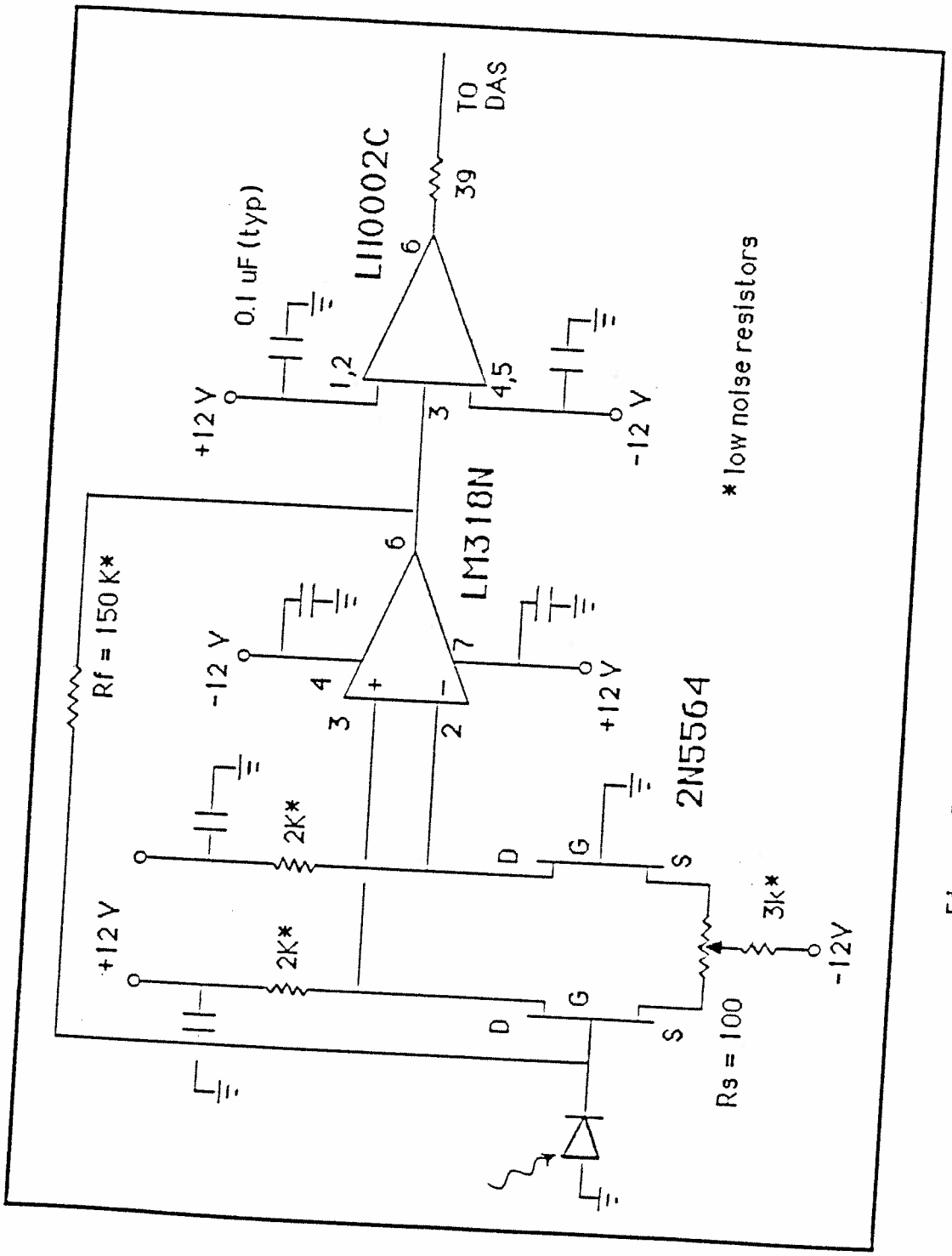

Figure 5 Amplification System

CHAPTER FOUR: DISCUSSION OF RESULTS

A. Operating Conditions

Luminosity data were collected under a variety of operating conditions. Fill pressures between 15 and 25 atm were invesitgated, as well as several propellant mixtures and a wide range of projectile velocities. Some of these mixtures, the operating velocity ranges, acoustic speeds, and theoretical detonation speeds are listed in Table 2.

Table 2: Typical Propellant Compostions

Propellant Mixture	Operational Velocity Range (m/sec)	Acoustic Speed (m/sec)	Chapman-Jouguet Detonation Speed (m/sec)
$2.5CH_4+2O_2+6N_2$	900-1600	362	1740
$4.5CH_4+2O_2+2He$	1300-1900	450	2080
$3.5CH_4+2O_2+6.5He$	1650-2100	555	2430
$3CH_4+2O_2+9He$	1900-2400	608	2700

The detonation speeds are determined from the zero thrust condition predicted by the theoretical model for 298°K and 25 atm.[1] When these mixtures are staged in successive segments of the ram accelerator tube (see Appendix A), a projectile can be propelled to velocities as high as 2400 m/sec.

The phenomena observed under these various conditions fall into distinct areas: thermal choking activity, and detonative phenomena. The results of these investigations are described below.

B. Transducer Signatures

Figure 6 displays the signatures of the pressure and electromagnetic (EM) transducers, and of the optical probe located at one of the stations in the ram accelerator test section. These signatures are typical of those produced by an accelerating projectile. The optical probe and transducers were located 30 cm from the entrance diaphragm for a segment containing $4.9CH_4 + 2O_2 + 6.5He$. The projectile velocity is ~1370 m/sec. Time is measured from the instant of DAS triggering.

The center trace corresponds to data obtained with the pressure transducer. The first pressure pulse is generated by the oblique shock system in the projectile's diffuser section. A series of pulses follow which increase the pressure to ~370 atm, after which the pressure decays. The sharp increase in pressure after the initial oblique shocks represents the normal shock, which is assumed to consist of a complex system of oblique and normal shocks similar to that observed in supersonic flows in long ducts.[23] The flow entering the combustion region is subsonic. The decay in pressure is caused by heat addition choking the flow and the subsequent, non-steady expansion of combustion products behind the thermal choking point.

The upper trace in Fig. 6 displays the output of the electromagnetic transducer. The zero crossing point of the first signal indicates the time of arrival of the magnetic ring located in the throat of the projectile. Similarly, the zero crossing point of the second signal identifies the rear of the projectile. These signals provide convenient reference points from which the position of the

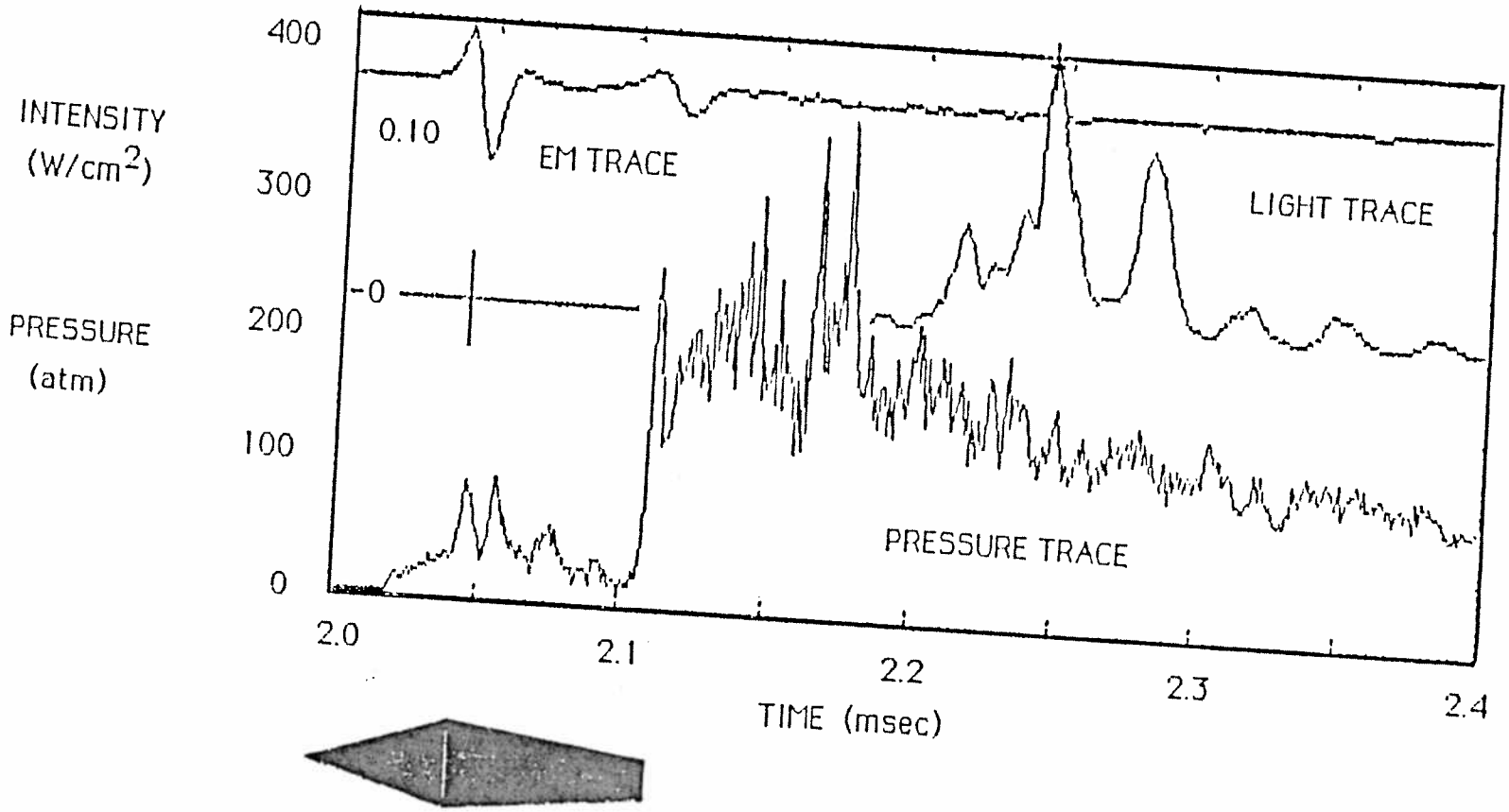

Figure 6 Transducer Signatures

shock system on the projectile and the location of the thermal choke point can be determined. A profile of the projectile scaled to the local velocity is shown beneath the traces to illustrate this point.

The bottom trace in Fig. 6 corresponds to the luminosity data obtained using a optical probe located at the same station as the pressure and EM transducers. In this particular shot, the luminosity begins ~120 μsec behind the throat of the projectile, or ~5 tube diameters. The intensity peaks a short distance later, at ~9 tube diameters, and then decays. The maximum intensity in this region is ~0.16 W/cm^2. The oscillations in intensity in the thermal choke region are attributed to the unsteady, turbulent behavior of combustion products. Recalling that total intensity is a function of temperature to the fourth power, the extreme oscillations in luminosity may result from relatively minor fluctuations in temperature in this region. Correlation with the pressure data shows that the normal shock system lies near the base of the projectile, and that the peak intensity occurred at the point where the pressure has fallen to approximately half its peak value, as predicted.

C. Preliminary Results

The data obtained during the initial phase of the optical investigation are similar to that shown in Fig. 6. The preliminary results, while not showing the same degree of resolution, did provide important information. The optical probe was able withstand the harsh environment in the ram accelerator tube. Light data was reliably collected under several operating conditions. What the model predicted

as a high-temperature choke point was observed to be a region of varying thickness. The data also indicated that the region of luminosity did not usually begin at the base of the projectile, but was typically located much further behind the projectile than originally anticipated. In addition, the position of this luminous region was perceived to be a function of projectile velocity in a given propellant mixture.

In addition to thermal choking activity, detonation phenomena were observed. However, it became apparent that the amplification system lacked sufficient frequency response to resolve much of the transient behavior. For example, the rise times of the normal shocks were often significantly less than for the light emission. Work was initiated to upgrade the amplification system to provide better frequency response and additional signal gain. During this time, the character of the light traces revealed more and more transient behavior for both detonation and thermal choking conditions. The final amplification system design, described in the previous chapter, allows the collection of light data which most closely matches the pressure histories. Oscillations in light emission are resolved where before none were indicated.

While much of the early work was devoted to proving the viability of the optical probe design, the investigation to date has supplied several interesting insights into thermal choking activity and detonations.

D. Thermal Choking Activity

In any given propellant mixture, the location of the luminous zone, or thermal choking region, is generally observed to fall further behind the projectile as it accelerates. The overall separation between the projectile base and the thermal choking point may reach as much as 15 tube diameters, depending on the length of the propellant stage and the total increase in projectile velocity. For instance, in a 3.9 m section of a propellant stage filled with $3.5CH_4 + 2O_2 + 6.5He$ at 25 atm, the length of the combustion zone grows an additional 1.5 tube diameters beyond the starting length of 3.1 tube diamters.

The effects of transition from one propellant mixture into another on the normal shock system has been described in the literature.[4] Based on the predictions of the analytic model, one would expect the velocity of the thermal choke point relative to the projectile to decrease during transitions. To investigate this phenomena, optical probes may be positioned at stations immediately before and after transition points. To date, none of the transient phenomena has been resolved.[2]

The effects of fill pressure on the length of the combustion zone have yet to be fully investigated, but preliminary results suggest increases in fill pressure cause the thermal choking region to move forward, closer to the base of the projectile. Further investigation with various velocity ranges and propellant mixtures is required.

On some occasions, a forward and backward excursion of the luminous zone, similar to that previously described for the normal shock system[2], has been observed. The factors relating these phenomena

are not fully understood and require further investigation. However, because the thermal choking is a fundamental element of normal shock stability, the optical probe will prove very useful in the future investigation of such behavior.

Another influence of increases in projectile velocity is a decrease in the maximum intensity of the light emission in the thermal choking region. For example, an increase in velocity of ~400 m/sec in a mixture of $4.9CH_4 + 2O_2 + 2He$ at 20 atm resulted in a ~75% drop in peak intensity. The width of the luminous zone is often seen to decrease as well. These phenomena, the extension of the combustion zone and the reduction in light emission, may be attributed to stretching of the flame front behind the projectile as its velocity increases. Acceleration of flame gases causes the interface between burned and unburned propellant to become thinner and longer, bringing about a reduction in energy radiation and thus the observed luminosity.[24]

In addition to the influence of projectile velocity on thermal choke region characteristics, there is also the factor of mixture chemistry. Each of the mixtures is selected to provide sufficient heat release to the flow and to constrain the projectile flight Mach number to within the range of ~2.5-4.5. This is achieved with the use of diluents, primarily nitrogen, helium, and excess methane.

Light data collected in the nitrogen mixtures at the lower end of the operating velocity range have often indicated the presence of a very long luminous zone which extends up to ~50 tube diameters behind the projectile. Compared with data obtained in a helium diluent

mixture for approximately equal velocities, the length of the combustion zone is typically similar. However, the intensity in the latter mixture is generally much greater. The helium mixtures have higher heat release values than the nitrogen mixture, and are also more fuel rich. This contributes to greater soot concentration in the combustion zone, which when combined with the higher wake temperatures causes the increased emission. This overall difference in intensity is observed throughout the shared velocity range of the mixtures. The differences in separation between projectile and luminous zone point to a projectile velocity influence, while the difference in emission intensity may be attributed to the higher heat release.

One other phemonenon observed to date is an asymmetry in luminosity pulses. Light data collected with opposing optical probes have shown some lag between similar peaks in emission. One possible explanation for this is swirling of the radiating carbon particles in the wake of the projectile. Further investigation is required to arrive at a more comprehensive understanding of this phenomenon.

E. Detonation Phenomena

The optical probe successfully provided light data during occasions of projectile unstart and propellant detonation.

Figure 7 shows pressure and light traces obtained in a mixture of $3.0CH_4 + 2O_2 + 9He$ at 25 atm. The lower trace was generated by a pressure transducer located 1.14 m from the entrance diaphragm. The steep rise in pressure to ~990 atm is associated with the normal shock. A corresponding rise in light emission occurs just behind the leading

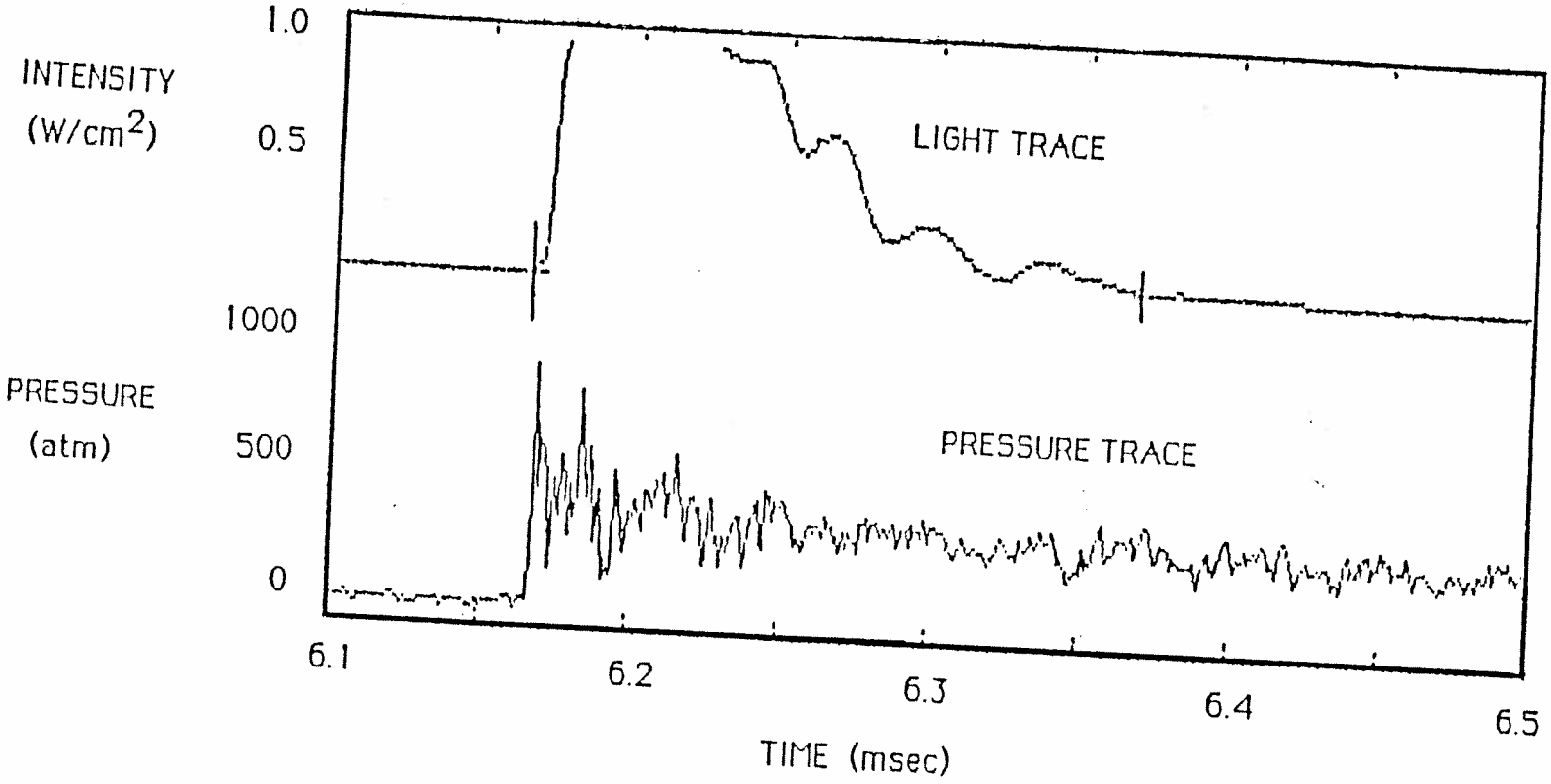

Figure 7 Detonation Wave

edge of the shock wave, as shown by the upper trace. The signal clipping resulted from insufficient attenuation with neutral density filters. A highly luminous zone extends ~50 tube diameters behind the shock front. The intensity here is estimated to be ~1 W/cm^2 or more.

The data presented in Fig. 7 are typical of that obtained for a variety of propellant mixtures and detonation wave velocities. In the beginning stages of detonation, some separation between shock front and luminosity has been observed. These observations suggest that an unstart sweeps over the projectile without immediately inducing detonation of the propellant gases. Within a few tube diameters, the flame front catches up to the high-velocity shock wave. In this phase, pressure and luminosity are observed to rise concurrently. One possible cause of detonative unstarts is communication between the separated boundary layer on the projectile and the combustion zone, which allows the combustion to creep forward on the projectile body. Light data from several shots have shown such a progression of the luminous combustion zone up and over the projectile. A strong shock, coupled with a highly luminous reaction front, is then observed to preceed the projectile. Figure 8 shows pressure and light data obtained in the region of the formation of a detonation wave. An unstart has just passed over the body of the projectile, which at the previous station in the ram accelerator tube was still accelerating normally. The luminous combustion zone, previously well behind the normal shock system on the accelerating projectile, has moved forward, accelerating toward the normal shock. Peak intensities on the order of ~0.18 W/cm^2 were observed. Detonation occurred shortly thereafter.

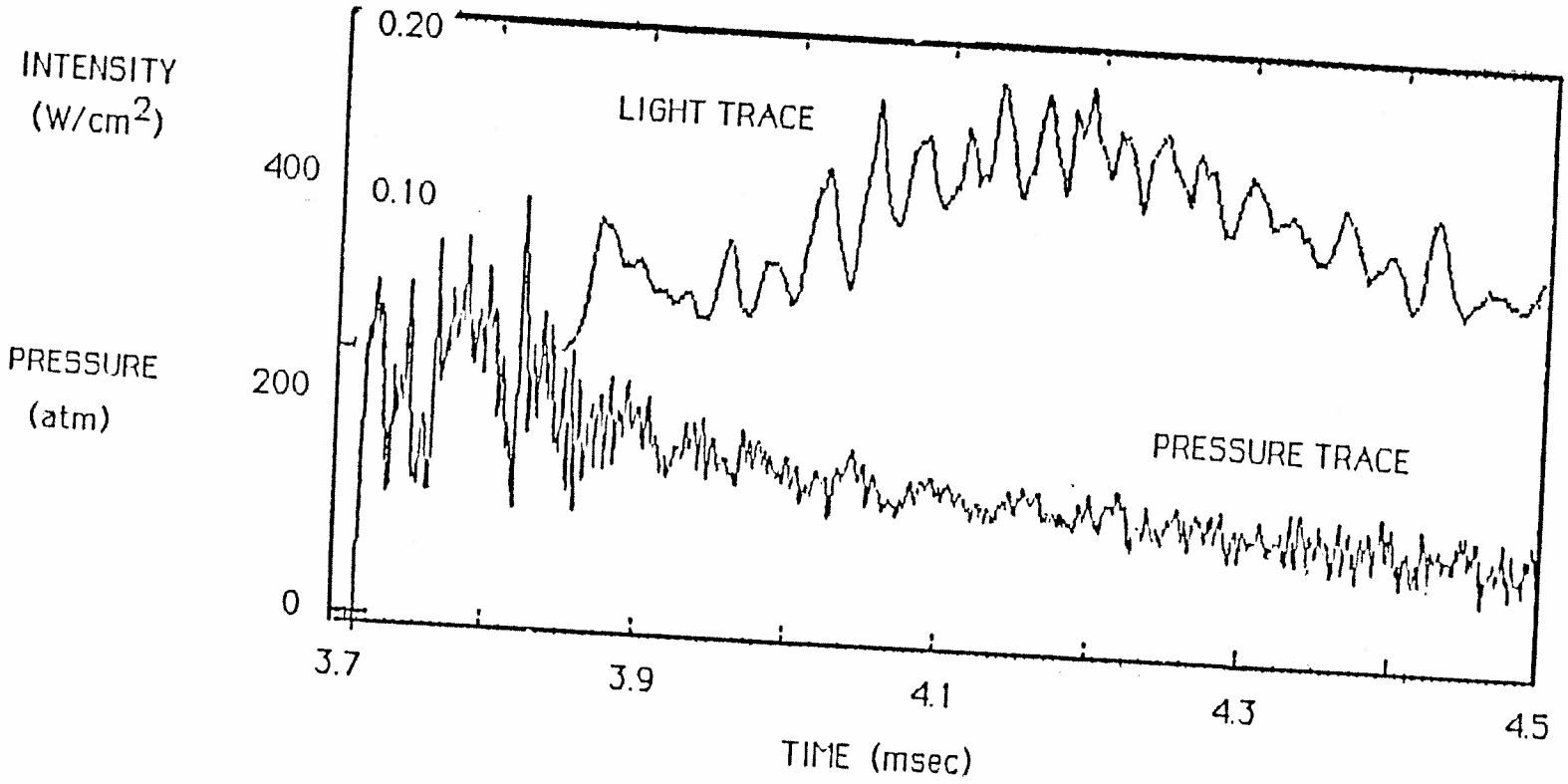

Figure 8 Unstart and Detonation

The light emission is produced by the shock-heated propellant gases and blackbody-like combustion products. One source of visible chemiluminescence in detonation of hydrocarbon fuels like methane is the three-body recombination reaction,

$$CO + O + M \rightarrow CO_2,$$

where M is any molecule or atom in the surrounding gas flow.[25] This type of chemiluminescence is assumed to contribute a greater share of the luminosity of detonation waves, however the relative amount is yet to be determined.

The response of the optical probe and amplification system to the normal overdriven detonation phenomena like that shown in the previous figures suggests that the optical probe will be useful identifying shock activity associated with the oblique detonation propulsion concept. This concept is the focus of pending research at the University of Washington facility.

CHAPTER FIVE: SUGGESTED RESEARCH

Three areas of research which may be readily approached using the optical probe are temperature measurements, observation of spectroscopic data, and of oblique detonation propulsion phenomena.

A. Temperature Measurements

A relatively straight-forward method of estimating the flow temperature in the wake of the projectile is possible using the optical probe. Rather than attempt an absolute intensity measurement, it is more feasible to compare intensities observed at different wavelengths.[26,27] By selectively filtering the output of optical probes located at the same station, the relative intensity can be obtained. A quick calculation then provides an estimate of the temperature. This method would not require calibration with a thermal source. Using Wien's approximation for blackbody intensity for small λT typical of visible flame radiation:

$$i'_{\lambda b} = \frac{2C_1}{\lambda^5 \exp(C_2/\lambda T)}$$

where

$$C_1 = hc_o^2$$

$$C_2 = hc_o/k$$

h = Planck's constant

c_o = speed of light

k = Boltzmann's constant

λ = wavelength

T = temperature

Comparing the intensity relations for two different wavelengths, e.g., at wavelengths in the red and green regions of the spectrum,

$$R = \frac{i'_{\lambda b,r}}{i'_{\lambda b,g}} = \left(\frac{\lambda_g}{\lambda_r}\right)^5 \exp\left[\frac{C_2}{T}\left(\frac{1}{\lambda_g} - \frac{1}{\lambda_r}\right)\right]$$

$$\text{for } T \cong T_r \cong T_g$$

With the experimentally determined ratio of intensities, R, and the wavelengths determined by the filters used, the temperature can be calculated:

$$T \cong C_2\left(\frac{1}{\lambda_g} - \frac{1}{\lambda_r}\right) \cdot \left[\ln R + 5 \ln\left(\frac{\lambda_r}{\lambda_g}\right)\right]^{-1}$$

The temperatures obtained with this method would be upper limits; the emissivity of the soot-laden gases is less than 1 in all but ideal conditions.

B. Spectroscopic Data

Continuum emission from active species in the ram accelerator combustion region may be examined using the monochrometer described in Appendix B. In the visible range, chemiluminescence from such molecules as C_2^*, CH^*, and CO_2^* may be observed. To date, it has been verified that selective bands of light collected using an optical probe can be observed. Preliminary data in the range of 4300-5100Å have been obtained. Further investigation is required to correlate chemiluminescent data with gasdynamic phenomena and propellant characteristics.

C. Oblique Detonation Phenomena

The oblique detonation propulsion concept, and related theoretical investigations, are described in Refs. 2, 4, and 5-7. Briefly summarized, the concept involves the detonation of the propellant gases by a reflected oblique shock originating at the nose of the projectile. The induced detonation wave on the shoulder of the projectile produces forward thrust. A schematic of the concept is shown in Fig. 9.

Investigation of this propulsion mode of the ram accelerator will rely on the optical probe to determine both the position and character of the driving shock system. Results from preliminary experimentation with the oblique mode show bow shocks originating at the nose of the projectile, as well as shock-induced detonation behind the throat. Projectile acceleration at high Mach numbers may contribute greatly to the increased luminosity of this mode.

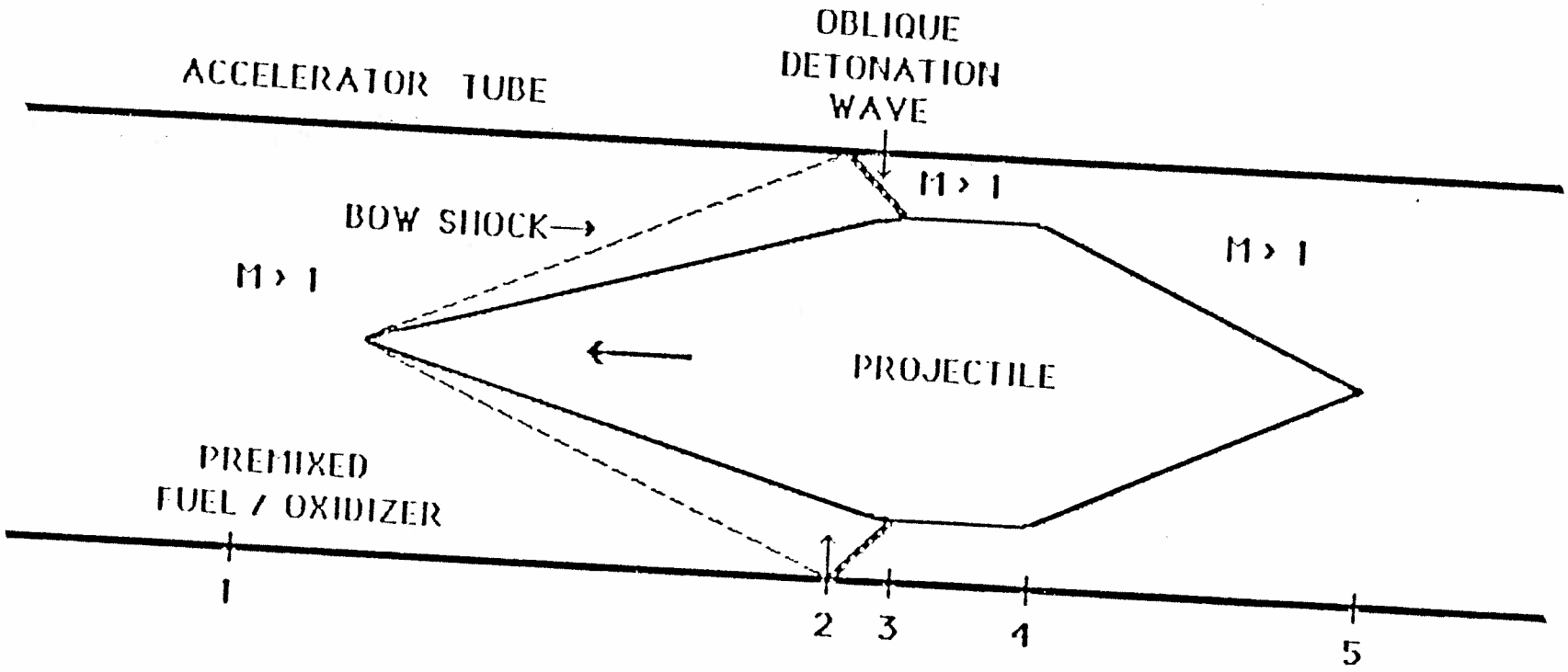

Figure 9 Oblique Detonation Mode

CHAPTER SIX: CONCLUSIONS

An optical probe has been developed to observe visible light radiation generated by ram accelerator wave and flame phenomena. The probe is able to withstand extreme temperatures and pressures while supporting the investigation of many related phenomena.

Using high-frequency light data, the correlation of luminosity with projectile-generated pressure waves and projectile position is achieved, adding to the current understanding of ram accelerator operation. The model of a flame-holding projectile base is supported by data obtained in a variety of test conditions. For a given propellant mixture, peak intensities are generally observed to decrease with increasing projectile velocity. Typical combustion zone dimensions are on the order of 3-10 tube diameters, increasing with increasing projectile velocity. Detonation waves are distinguished from other luminous phenomena by their fast rise times and extreme brightness.

The optical probe may be used to investigate subsequent modes of operation, measure flow temperatures, and collect spectroscopic data, as well as examine thermally choked combustion activity.

The transmission of light data can be increased by the addition of fiber and photodiode alignment guides, improved polishing techniques, and the use of glass fiber optics. The frequency response and gain of the amplification system are adequate. Improved alignment of neutral density (and color) filters will reduce reflection and scattering losses at the interface between fiber and photodiode surfaces.

LIST OF REFERENCES

1. Bruckner, A.P., Knowlen, C., Scott, K.A., and A. Hertzberg, "High Velocity Modes of the Thermally Choked Ram Accelerator," AIAA Paper 88-2925, AIAA/ASME/SAE/ASEE 24th Joint Propulsion Conference, Boston, MA, July 11-13, 1988.

2. Hertzberg, A., Bruckner, A.P., and D.W. Bogdanoff, "Ram Accelerator: A New Chemical Method for Accelerating Projectiles to Ultrahigh Velocities," AIAA Journal Vol. 26 (February 1988), 195-203.

3. Knowlen, C., Bruckner, A.P., Bogdanoff, D.W. and A. Hertzberg, "Performance Capabilities of the Ram Accelerator," AIAA Paper 87-2152, AIAA/SAE/ASME/ASEE 23rd Joint Propulsion Conference, San Diego, CA, June 29-July 2, 1987.

4. Bruckner, A.P., Bogdanoff, D.W., Knowlen, C. and A. Hertzberg, "Investigations of Gasdynamic Phenomena Associated with the Ram Accelerator Concept," AIAA Paper 87-1327, AIAA 19th Fluid Dynamics, Plasma Dynamics and Lasers Conference, Honolulu, HI, June 8-10, 1987.

5. Hertzberg, A., Bruckner, A.P., Bogdanoff, D.W. and C. Knowlen, "The Ram Accelerator and its Applications: A New Chemical Method for Reaching Ultrahigh Velocities," Invited Paper, 16th International Symposium on Shock Tubes and Waves, Aachen, West Germany, July 26-30, 1987.

6. Bruckner, A.P., Hertzberg, A., Knowlen, C., and D.W. Bogdanoff, "Investigation of Gasdynamic Phenomena in the Ram Accelerator," Journal of Propulsion and Power, in press.

7. Brackett, D.C. and D.W. Bogdanoff, "Computational Investigation of Oblique Detonation Ramjet-In-Tube Concepts," Journal of Propulsion and Power, in press.

8. Gaydon, A.G. and H.G. Wolfhard, Flames: Their Structure, Radiation, and Temperature, 4th ed. (London: Chapman Hall, 1979), 268-290.

9. Crosley, D.R., ed. Laser Probes for Combustion Chemistry ACS Symposium Series 134 (Washington, DC: American Chemical Society, 1980).

10. Kimball-Linne, M.A., Kychakoff, G., and R.K. Hanson, "Fiberoptic Adsorption/Fluorescence Combustion Diagnostics," Combustion Science and Technology Vol. 50 (1986), 307-322.

11. Shapiro, A.H., The Dynamics and Thermodynamics of Compressible Fluid Flows Vol. I (New York: Ronald Press, 1953), 195-201.

12. Shapiro, 83,84.

13. Zukowski, E.E. and F.E. Marble, "Experiments Concerning the Mechanism of Flame Blowoff from Bluff Bodies" in Proceedings of the Gasdynamics Symposium on Aerothermo-Chemistry, ed. D.K. Fleming (Evanston, Il.: Northwestern University, 1956), 205-209.

14. Gaydon, A.G., The Spectroscopy of Flames (New York: John Wiley Sons, Inc., 1957), 4.

15. Siegal, R. and J.P. Howell, Thermal Radiation Heat Transfer, 2nd ed. (New York: Hemisphere Publishing Corporation, 1981), 598.

16. Gaydon and Wolfhard, 202, 206.

17. Ibid.

18. Dodge, L.G., "Optical Adsorption and Emission Measurements," Experimental Diagnostics in Gas Phase Combustion Systems, ed. Ben T. Zinn (Princeton: Princeton University, 1977), 161.

19. Gaydon and Wolfhard, 259.

20. Dodge, 161.

21. Dodge, 160.

22. Siegal and Howell, 659, 667.

23. Shapiro, 135-137.

24. Gaydon, 165, 166, 173.

25. Sokolik, A.S., Self Ignition, Flame, and Detonation in Gases. Translated from Russian by N. Kaner, ed. R. Hardin (Jerusalem: Israel Program for Scientific Translation, 1963), 347; available from the Office of Technical Services, U.S. Dept. of Commerce, Washington, D.C.

26. Dodge, 160.

27. Siegal and Howell, 659, 667.

28. Seigel, A.E., "Theory of High-Muzzle-Velocity Guns," Interior Ballistics of Guns, eds. Krier, H. and M. Summerfield, Progress in Astronautics and Aeronautics, Vol. 66 (New York: American Institute of Aeronautics and Astronautics, 1979), 135-175.

APPENDIX A: EXPERIMENTAL FACILITY

A. Test Facility

The experimental facility, designed to demonstrate proof-of-principle of the ram accelerator concept and to confirm theoretical predictions, is illustrated in Fig. 10. The principle components are the single-stage light gas gun, ram accelerator test section, final dump tank, and projectile decelerator. Associated gas handling and vacuum systems are not indicated. The light gas gun, of conventional design[28], is employed to accelerate the projectile and a launching sabot (typical combined mass ≅ 70 gm) to speeds up to approximately 1300 m/sec. The muzzle of this gun is connected to a perforated-wall tube which passes through an evacuated dump tank, where the helium driver gas is dumped.

After travelling through the dump tank, the projectile/sabot combination enters the ram accelerator test section. This section is comprised of seven steel tubes made from heat-treated 4150 alloy. All seven tubes have a 38 mm bore and a 100 mm outer diameter. The tubes were constructed in 1.22 and 2.44 m lengths. The overall length of the test section is 12.2 m.

A total of 32 pairs of diametrically opposed instrumentation ports are distributed at regular intervals in the test section. The short tubes have four pairs of instrumentation ports tapped at 30.5 cm intervals. Interval spacing in the longer tubes is 61.0 cm. At four axial stations there is an additional pair of opposed ports positioned at right angles to the other ports. This permits the simultaneous use of four transducers at each of those locations. The instrumentation

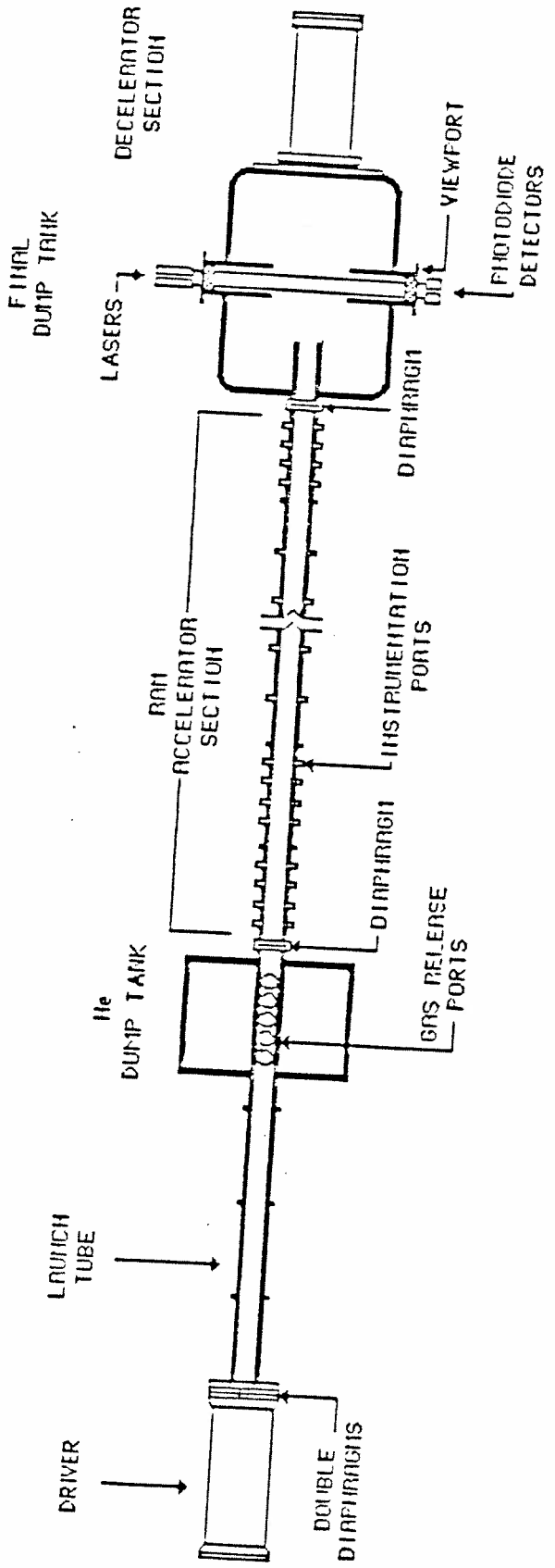

Figure 10 Ram Accelerator Facility

ports house piezo-electric pressure transducers, electromagnetic coil transducers, and optical probes. The test section is designed to operate at propellant fill pressures up to 50 atm. Nominal fill pressures of 25 atm result in peak drive pressures up to 10,000 psi on the projectile. The test section entrance and exit are closed off using thin Mylar diaphragms, typically 14 mil thick. These diaphragms are also used to separate, or stage, different propellant mixtures. Up to five such stages, of varying length, can be employed.

When the projectile leaves the test section, it passes through a 76 cm long drift tube, and then flies free through the evacuated final dump tank. The dump tank is equipped with opposing viewports for spark photography and two-beam laser velocity measurements. The projectile is brought to a stop in a decelerator tightly packed with rug remnants.

B. Projectile Configuration

The nominal projectile geometry is illustrated in Fig. 11. The projectile is fabricated from magnesium in two pieces, the nose cone and body with integral fins. The nose half-angle is 12.5 degrees. The fins serve only to center the projectile as it travels through the tubes. Between the nose and body a thin magnetic disk is inserted. A second magnet can be placed at the rear of the projectile. The magnets interact with the electromagnetic coil transducers to provide position data. The length of this projectile is 13.7 cm; the maximum diameter is 2.89 cm, which results in a diffuser area ratio of 2.37. The mass of the projectile is typically about 57 gm; the launching sabot, 13 gm. In some of the experiments projectiles with 10-degree nose half angles

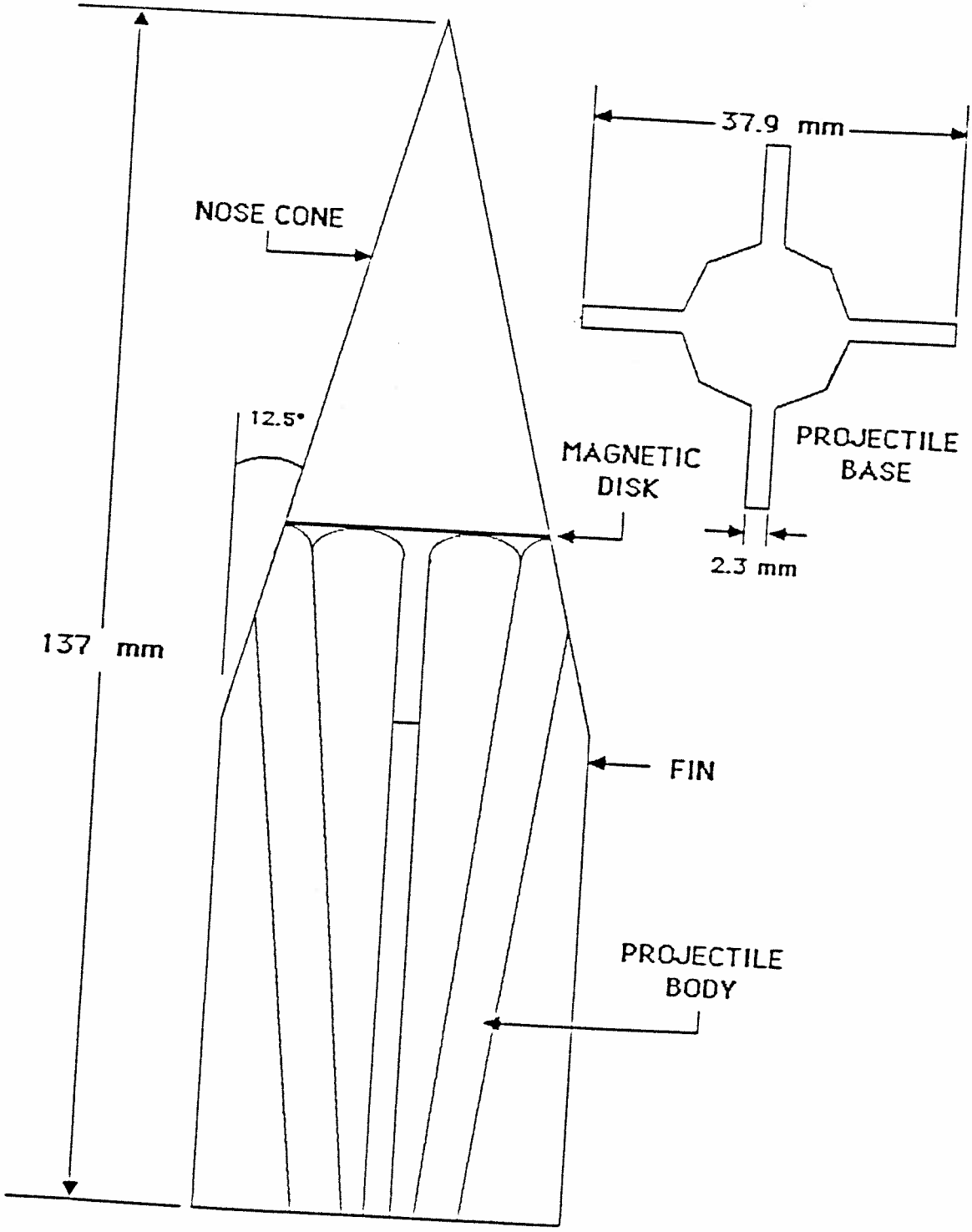

Figure 11 Projectile Configuration

and 1.3 cm longer bodies have been used. Other variations in projectile geometry include base diameter, fin shape and length, and additional body length changes.

C. Gas Handling System

Commercial bottled helium provides the driver gas supply. A diaphragm pump (Corblin, model A34-G400) capable of reaching 400 atm is used to attain the high pressures required by the light gas gun. A Sargent-Welch vacuum pump (model 1398) is employed to evacuate the launch tube, dump tanks, and test section. Commercial bottled methane, oxygen, and diluent gases are used to mix the gaseous propellant. These gases are filtered, metered using sonic orifices, sent through a mixing chamber, and then routed to stages in the test section. By adjusting the feed pressures of the various constituents, the desired mixture ratios are obtained. The mixing system is regularly calibrated.

The bottled gases are housed in a bunker. An additional bunker houses personnel, vacuum and gas mixing panels, the high-pressure pump, the vacuum pump, and the data acquisition system.

APPENDIX B: INSTRUMENTATION AND DATA ACQUISTION SYSTEM

A. Transducers

Both Kistler model 211B1 and PCB model 109A pressure transducers have been used to capture the pressure history. Figures 12 and 13 contain schematics of the nominal configurations of both probes. Typically, a pressure transducer is mounted directly opposite one of the custom-made electromagnetic coil transducers, which are used to indicate the position of the projectile. These position data are independent of the disposition of the pressure waves generated by the projectile. A schematic of the electromagnetic transducer is shown in Fig. 14.

B. Monochrometer

At one of the instrument ports in the test section, the light data emitted from an optical probe may be collected and directed at the entrance slit of a Spex 0.22 m monochrometer (Minimate, model 1670). The schematic in Fig. 15 shows the layout of the monochrometer, fiber, and optical probe. The monochrometer is equipped with a 1200g/mm diffraction grating with a blaze angle at 300 nm. The entrance slit width could be continuously adjusted between 1 μm and 3 mm; an entrance slit shutter can be configured for full slit height (20 mm), and 10 and 2 mm heights.

Wavelength readout is displayed on a digital counter with 1 Å gradations. With a 1200g/mm grating, a 2.5 mm slit width corresponds to a 5 nm bandpass.

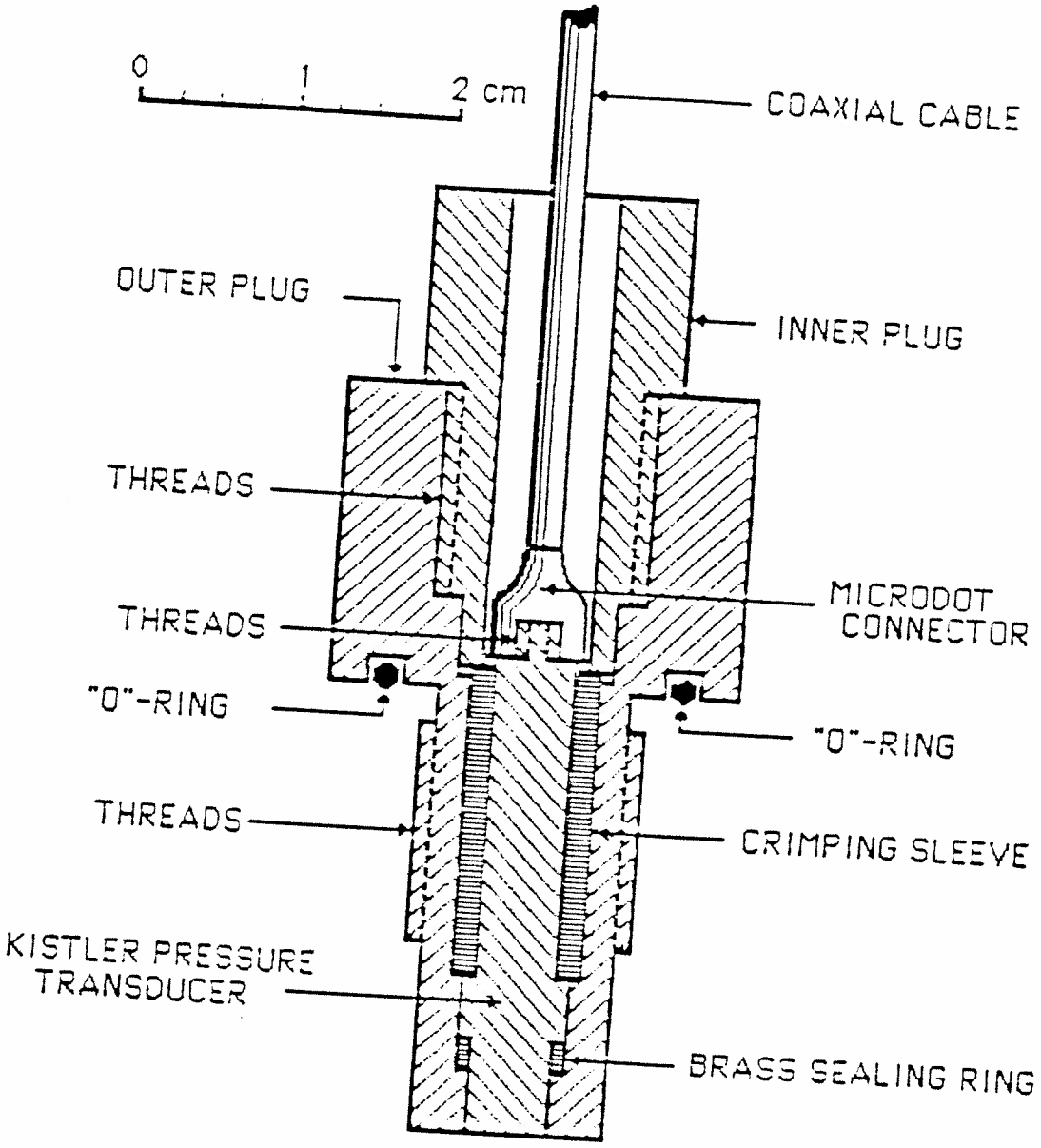

Figure 12 Kistler Pressure Transducer

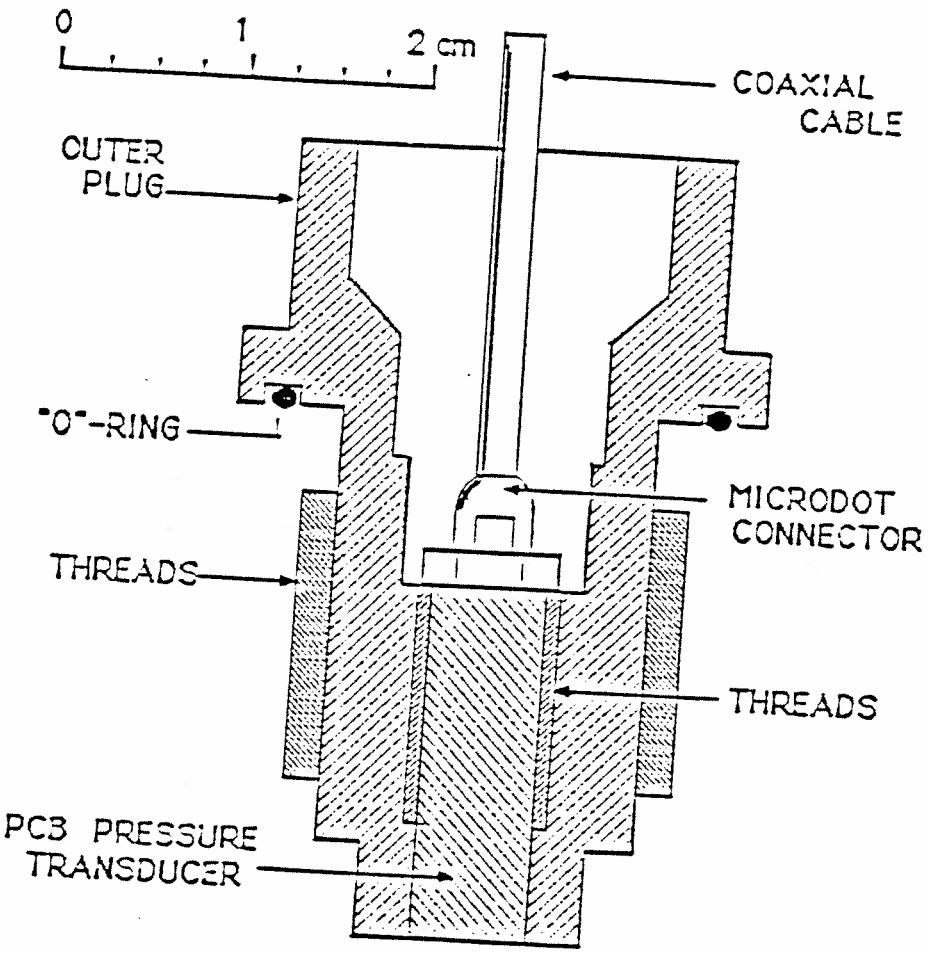

Figure 13 PCB Pressure Transducer

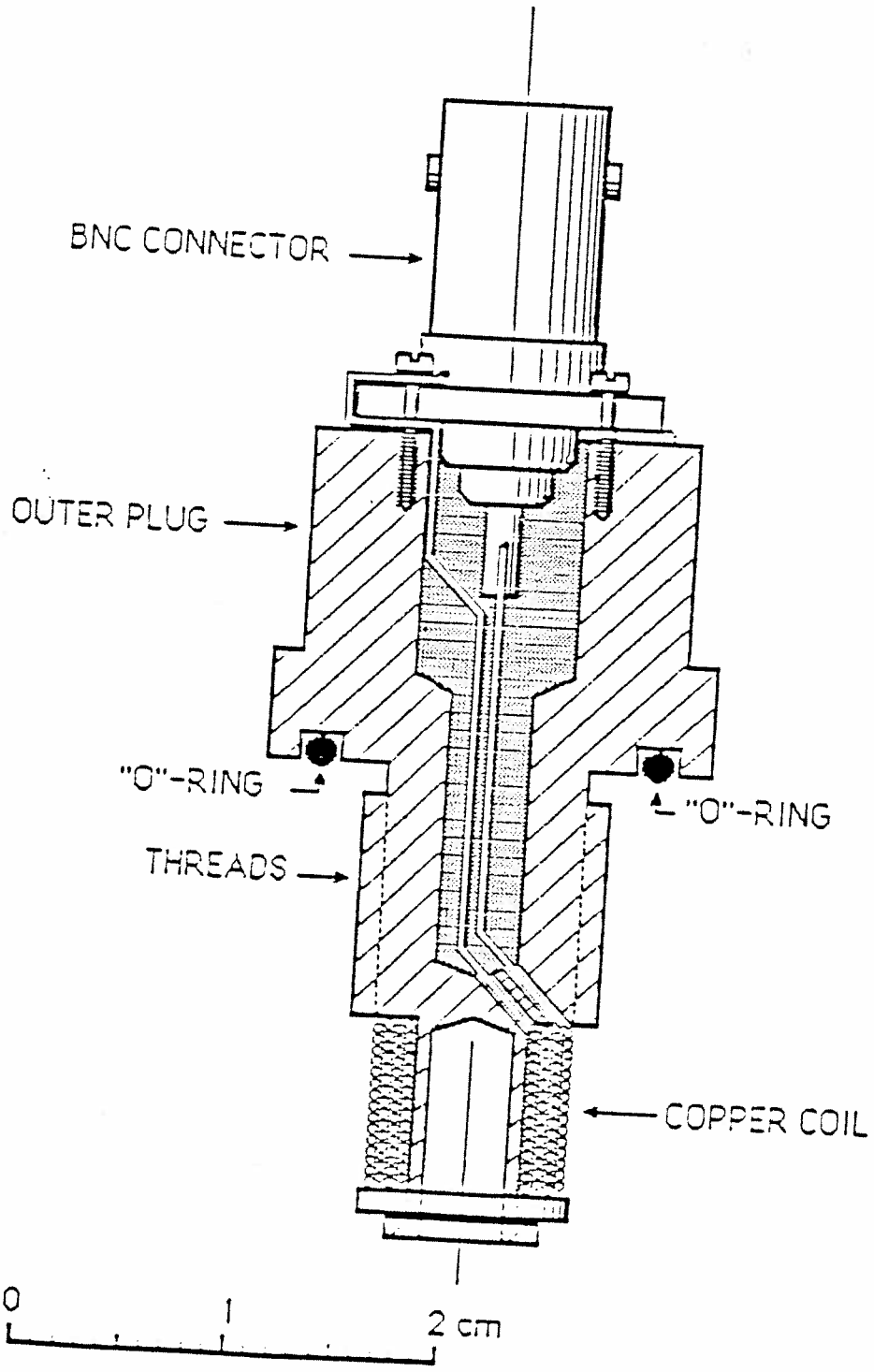

Figure 14 Electromagnetic Coil Transducer

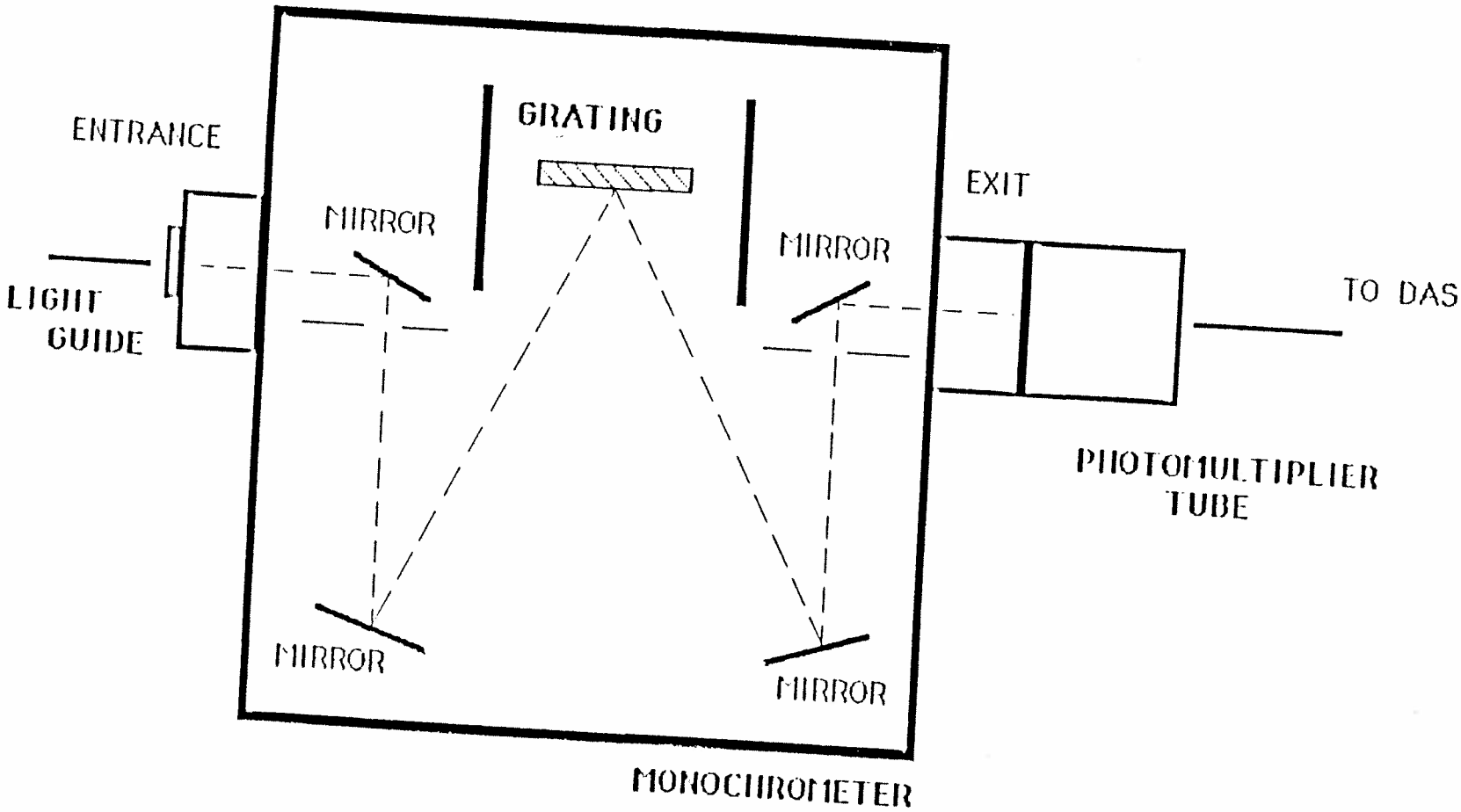

Figure 15 Monochrometer System

A photomultiplier tube (RCA 331039) is contained in the exit slit housing to detect any light emitted from the monochrometer. The output of the photomultiplier is then directed to the data acquisition system.

The monochrometer wavelength readout is calibrated using a low-pressure Mercury/Argon gas lamp (Oriel model 6035).

C. Data Acquisition System

A 20-channel Le Croy Research Systems Corp. data acquisition system (DAS) is used to process data from the pressure and electromagnetic transducers, and from the optical probes. Data signals are conducted through co-axial cables to Quad 10-bit transient digitizers (Le Croy model 8210). Four analog signals per module are digitized using track and hold circuits, then stored in five memory modules (Le Croy model 8800A) which each have a capacity of 32,000 12-bit words. Each module can be addressed separately; the data are read through the memory control circuits in the 8210 units.

A Le Croy model 8252 32-channel data logger, Le Croy model 8910A CAMAC to GPIB interface, and the memory modules are contained in a Le Croy model 1434 CAMAC crate. This crate uses a model 1034P CAMAC power supply.

The CAMAC to GPIB interface is connected to an IBM PC-XT microcomputer, which has a 128kB random access memory, a 40kB read-only memory, a 10MB hard disk, and a 360kB floppy-disk drive. To manipulate and display the data a Le Croy Wave-form Catalyst Software program is used. Formatted data are printed using a Hewlett-Packard HP2225C Think Jet printer. Figure 16 contains a schematic of the DAS.

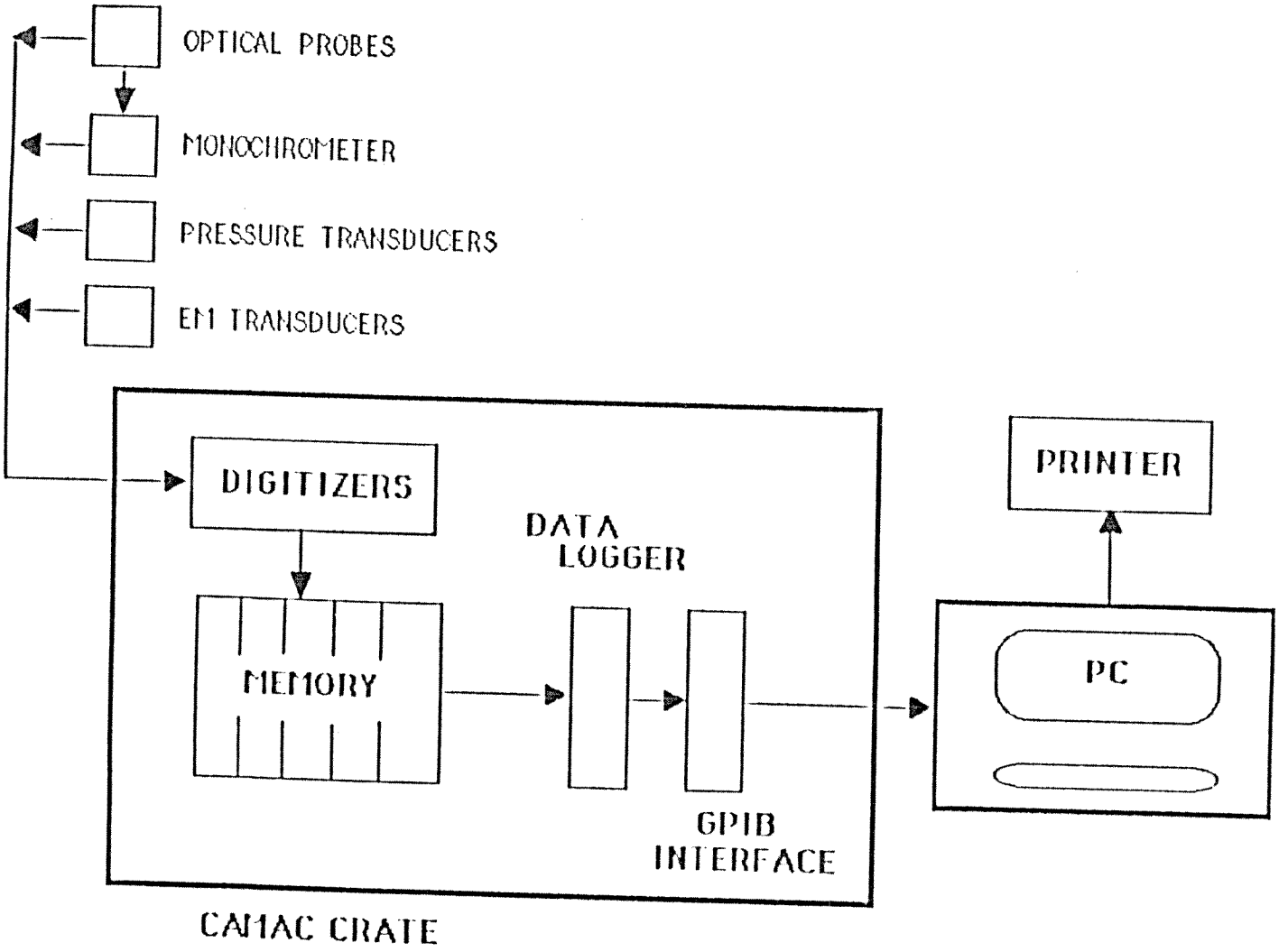

Figure 16 Data Acquisition System Schematic